Long-Term Seismic Activity and Present Microseismicity on Active Faults in Southwest Japan

Tameshige TSUKUDA

Disaster Prevention Research Institute, Kyoto University, Uji, Kyoto, Japan

(Received October 23, 1984)

Abstract. Excavations across several active faults in southwest Japan have disclosed a series of large geologically recent earthquakes for each fault studied. Recurrence intervals range from 1,000 to 20,000 years for the Shikano, Yamasaki, Umehara, Atotsugawa, and Atera faults. Strong irregularity in the intervals is found for the Umehara fault, one of the 1891 Nobi earthquake faults. Activity on the Atotsugawa and Atera faults, two large conjugate faults, seems to be coupled. Some geologically estimated events coincide well with the historical earthquakes.

Microearthquake distribution on and around an active fault seems to depend on the mode of the latest large earthquake associated with the fault and the lapse of time from it. Difference of microseismic pattern around individual faults may reflect different stages in an earthquake cycle of a several-thousand-year period. Relatively large aseismic regions of 20-km diameter, found on both the Yamasaki and Atotsugawa faults, may be where the stresses were almost completely released during the latest large slip events about 1,100 and 120 years ago, respcetively.

A series of large earthquakes represents a long-term behavior of an active fault, while medium-scale earthquakes and microseismic patterns provide a medium-term activity. The 3–4 year period fluctuation in the microseismic activity around the Yamasaki fault is one of short-term characteristics.

1. Introduction

Precise knowledge of time dependent properties of active faults is becoming increasingly important in estimating earthquake risk in a region of active faults.

Long-term activity of a fault is characterized mainly by time intervals between successive earthquakes that ruptured the entire fault or the greater part of it. With the average recurrence interval and the occurrence time of the latest event, the dates of the future earthquakes would be predicted in a long timescale.

In an inter-seismic period of large earthquakes, we have a medium-term activity of smaller events including microearthquakes. Present-day microseismicity around the region of faults must have something to do with both the most latest and forthcoming large earthquakes originating from the faults.

The purpose of this paper is to show the geologically disclosed long-term nature of active faults in southwest Japan and to discuss the microseismicity around the faults in connection with the recent large earthquakes confirmed by the former study. The first part of this paper will be devoted to the review of the trenching studies of faults. This geological method (SIEH, 1978a, b, 1981) enabled us to get more direct and detail-

ed evidence of faulting than geomorphological estimations of slip rates. The second part will deal with distribution of active faults and related microseismicity. Emphasis will be place on how the distribution pattern of microearthquakes differs frrom fault to fault. In the third part, we will try to quantify the medium-to-short term microseismic activity by the use of data from a long-running observation of 18 years. Finally, we will present tentative interpretations of long-, medium-, and short-term fault activities in terms of spatial and temporal patterns of seismicity.

The target area in this paper is shown in Fig. 1. The region in and around the Kinki and Chubu districts has the most dense population of active faults, and the historical seismicity shows that the probability of causing damaging earthquakes in that region is about twice as high as the average in the whole inland of Japan (MAT-

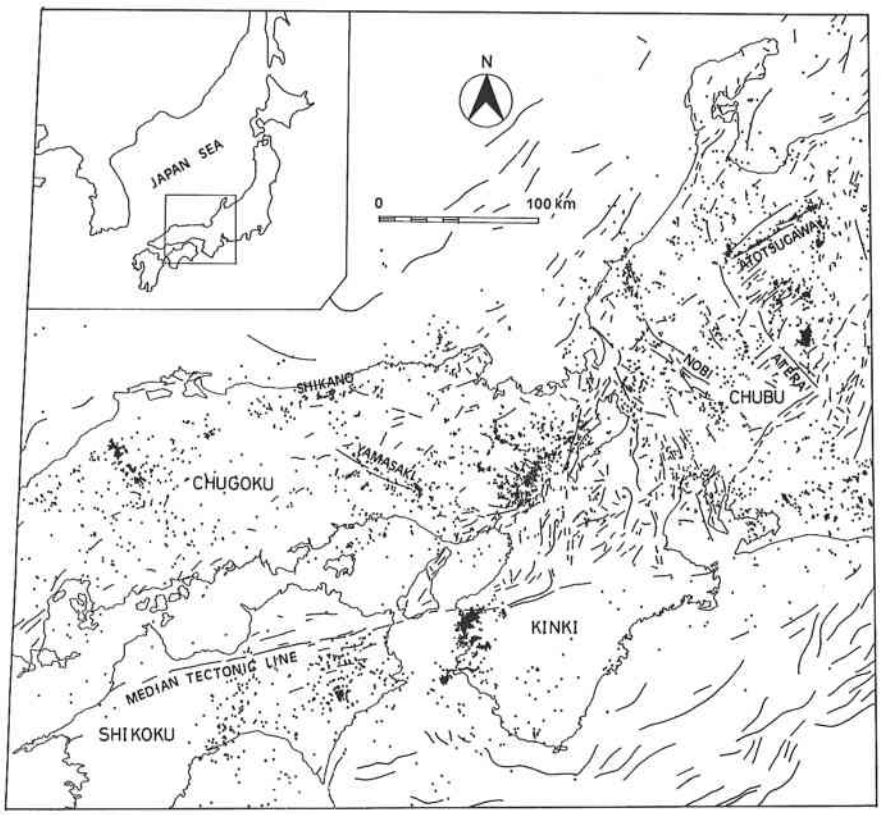

Fig. 1. Distribution of active faults and microearthquakes in the western part of Japan. Active faults together with active folds beneath the sea are mapped based mainly on a geomorphological interpretation made by the RESEARCH GROUP FOR ACTIVE FAULTS (1980a, b). Microearthquake foci with magnitude 1.0 or above are plotted putting together all the seismicity data in 1979 compiled by each observatory or observation center attached to universities (GROUP OF COMPILATION FOR MICROSEISMICITY OF JAPAN, 1979, 1983). Trenching researches were conducted at the Shikano, Yamasaki, Nobi, Atotsugawa and Atera faults.

SUDA, 1980, 1981). Relevant active faults are the Shikano, Yamasaki, Nobi, Atotsugawa and Atera faults (or fault systems). All of them are mainly strike-slip faults with a small amount of dip-slip component.

We will show that the long-term seismic cycle there is more than 1,000 years, and that duration time of a medium term activity following the main event is more than 100 years. The short-term recurrence time of microseismic fluctuations in the Yamasaki fault region is several years. It is generally difficult to say where we should distinguish short-term from medium-term in the time range. We will use "short-term" for a several-year-peiod variation of microseismicity.

2. Long-Term Activity Disclosed by Trenching

Trenching excavation is a method to find out minor faults, which are sometimes extremely small, cutting young sediments covering an active fault and to constrain the dates of slip by dating the strata. The first successful application of this method was made by SIEH (1978a). He found the fairly repetitive fault activity at the south-central segment of the San Andreas fault. OKADA *et al.* (1981b) applied this method to the Shikano fault (See Fig. 1), the source of the 1943 Tottori earthquake, and found that the second latest magnitude-7-class event occurred 6,000±2,000 years ago. It was the first attempt to find out an old earthquake by trenching in Japan. The following is a review of the trenching studies in southwest Japan. The site maps are given in Fig. 2. The name of trench, date of trenching, maximum size of trench and references are listed in Table 1. Summary of the constrained dates of earthquake events are given in Fig. 16.

Table 1. Excavations of active faults in southwest Japan. The size of the trench is given by the maximum lengths of its capacity. Trench A′ for the Yamasaki fault means the enlarged trench of A. In references, D.P.R.I., G.S., and R.G.A. denote Disaster Prevention Research Institute, Geological Survey of Japan, and Research Group for Excavation of the Atotsugawa Fault, respectively.

Name of Trench or Fault	Date of Trenching	Size of Trench (m)			References
		Length	Width	Depth	
Shikano A	Nov. 28–Nov. 30, 1978	10	2	2	OKADA *et al.* (1981b)
B	Nov. 28–Nov. 30, 1978	15	5	3.5	
C	Dec. 2, 1978	10	3	1.5	
Yamasaki A	Mar. 1–Mar. 5, 1979	25	5	3	OKADA *et al.* (1980, 1981a)
A′	Mar. 4–Mar. 5, 1979	25	5	5.5	
C	Mar. 2–Mar. 5, 1979	25	5	3	
Umehara (Nobi fault system)	Jul. 26–Aug. 6, 1981	26	8	5	D.P.R.I. (1983)
Neodani (Nobi fault system)	Aug. 4–Aug. 7, 1981	40	8	5	D.P.R.I. (1983)
Atera	Oct. 15–Oct. 30, 1981	25	11	8	G.S. (1982)
Atotsugawa	Jul. 19–Aug. 2, 1982	23	9	10	R.G.A. (1983)

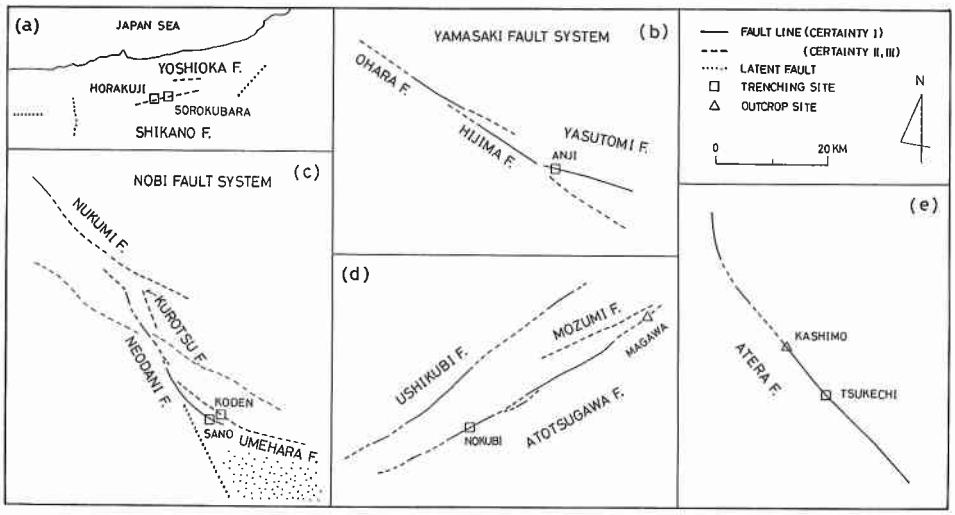

Fig. 2. Simplified fault map showing the locations of trenching sites. Solid lines show active faults with Certainty I, broken lines Certainty II or III (RESEARCH GROUP FOR ACTIVE FAULTS, 1980a, b). (a) Around the Shikano and Yoshioka faults: dotted lines indicate latent faults or fractured zones estimated by microearthquake distributions. (b) Yamasaki fault system. (c) Nobi fault system: dotted line indicates the latent earthquake fault of 1891 estimated by levelling and triangulation (MIKUMO and ANDO, 1975). Microearthquakes concentrate on the region around this fault and the Umehara fault. Shadow indicates high microseismic region. (d) Atotsugawa fault: The outcrop at Magawa was studied by TAKEMURA and FUJII (1983). (e) Atera fault: The outcrop at Kashimo was studied by HIRANO and NAKATA (1981).

2.1 Shikano fault

We selected two sites, Horakuji and Sorokubara (Fig. 2), which are 3 km apart from each other along the Shikano fault. Both of the sites are in paddy fields. At Horakuji, several kilometers west of the center of the fault, two trenches, Trench A and B, were constructed in parallel, separated only by 23 m, across the fault. The very fault line was bale to be exactly traced by connecting the points where surface displacements associated with the 1943 Tottori earthquake (M7.4) had remained as it was until the end of 1978, the time of the trenching. At Sorokubara (Trench C), we estimated the very points based on the words by the owner of the paddy field saying that the displacements at the time of the Tottori earthquake took place crossing the center of his field.

The disturbance of the geologic section due to the 1943 earthquake, the latest event, was recognized in the form of minor faults and open tunnel in Trench A (Fig. 3), and offsetting by flexure of a black humic bed (Layer B5 in Fig. 4) in Trench B. The horizontal width of the disturbance was within 1.5 m.

The second latest event was confirmed by the flexure of a sand bed, including a small amount of humic soil, offset vertically by more than 1.3 m with the southern side up at Trench A (Layer A7), and by the fault disrupting the lower black humic

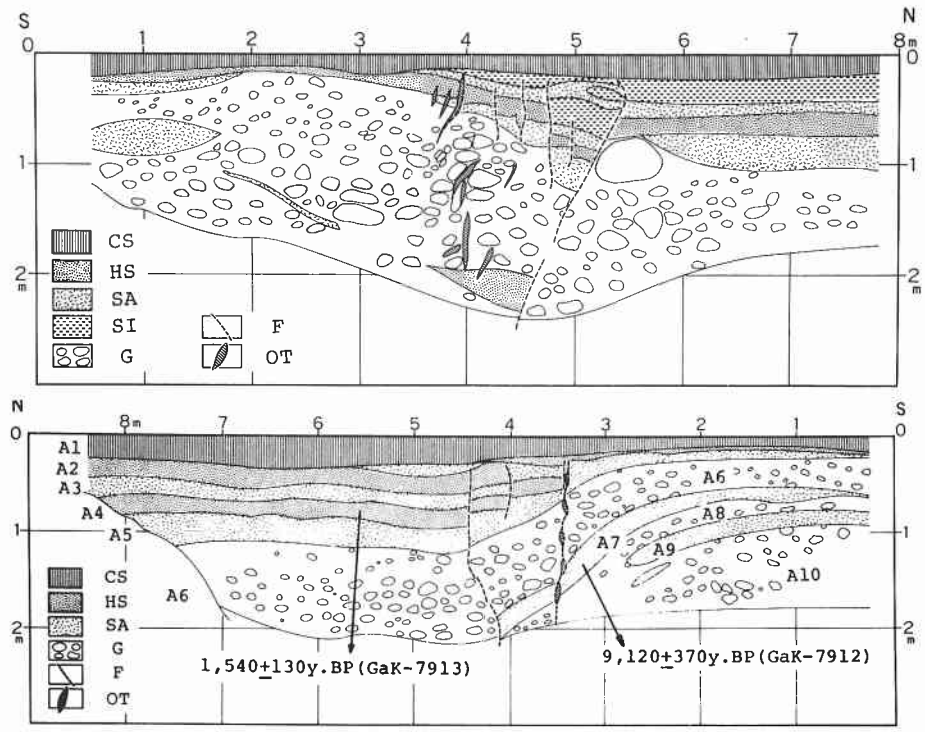

Fig. 3. Geologic section of Trench A, Horakuji, the Shikano fault (Upper: west wall, Lower: east wall). CS: cultivated soil, HS: humic soil, SA: sand, SI: silt, G: gravel, F: fault, OT: open tunnel. A1 to A10 are layer numbers. Numerals indicate ^{14}C dates with sample numbers.

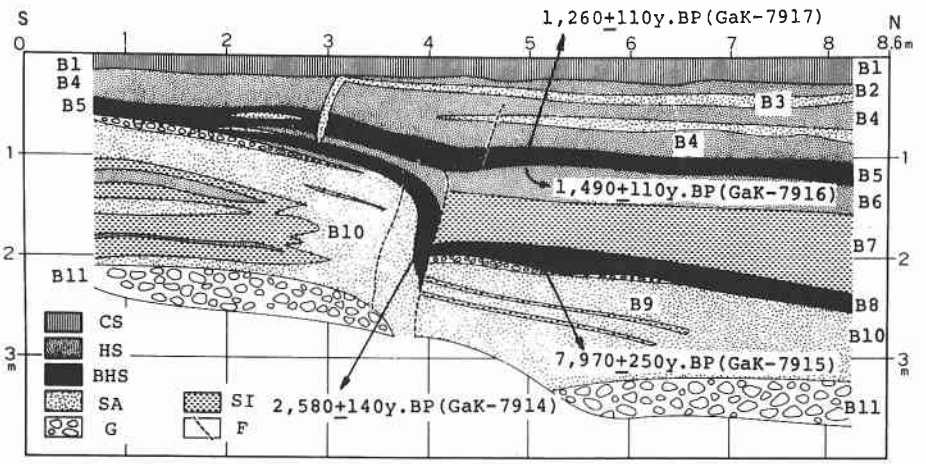

Fig. 4. Geologic section of Trench B, Horakuji, the Shikano fault (west wall) as similarly as Fig. 3. BHS: black humic soil.

soil with a vertical gap northern side down of 1.0 m at Trench B (Layer B8). The amount of those offsets is about twice that of the latest event, indicated by the flexure of the upper black humic bed on the wall of Trench B. This means that the older event should have had almost the same amount of slip as the younger one. The offset by a single event estimated by this trenching study is almost equivalent to the 50 cm surface displacement due to the recent destructive earthquake of 1943 (TSUYA, 1944).

^{14}C dates of the upper and lower humic soil layers (A4 and A7 for Trench A; B5 and B8 for Trench B) give the upper and lower limits of the data of the second latest event. Taking the results from the two trenches into consideration, we determined the date to be between 1,540 and 7,970 yrs B.P. Although we could not excavate to find more events other than the two mentioned above, the repetitive nature of events is suggested by the results of geomorphological and geological surveys along the Shikano fault (OKADA *et al.*, 1981b). Then, if we assume a periodicity in earthquake occurrence, the repeat time here would be 4,000–8,000 years.

At Trench C, we could not find any evidence relevant to the old events other than the 1943 event. Moreover, its geologic section was lacking fine grained young sediments, which might be brought away by flooding of a nearby river.

More details of the trenching and some related studies on the Shikano fault are presented in another paper (OKADA *et al.*, 1981b).

2.2 Yamasaki fault

The trench sites were located at the two small valleys in the western part of the Yasutomi fault, the eastern segment of the Yamasaki fault (See Fig. 2 and Fig. 5). We made four trenches, two in each valley. However, due to collapsing of the side walls, we could not observe two fo them well. Trench A was situated in the 160-m-long and 25-m-wide valley, where the stream was offset left-laterally by about 50 m

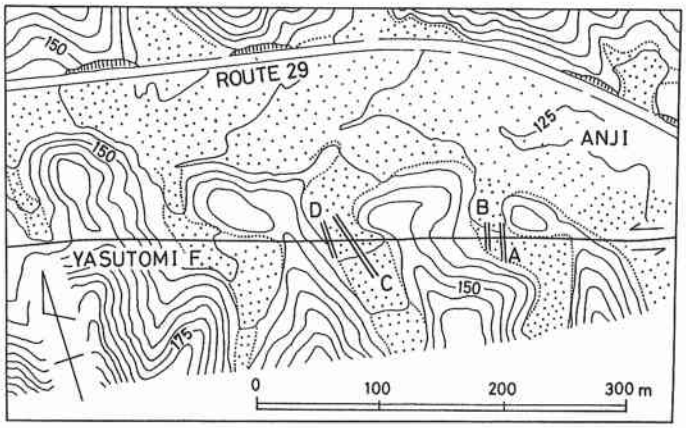

Fig. 5. Topographic map showing the locations of the trenches A, B, C and D at Anji, the Yasutomi fault (Yamasaki fault system). Note the left lateral offsetting of small ridges and valleys along the fault.

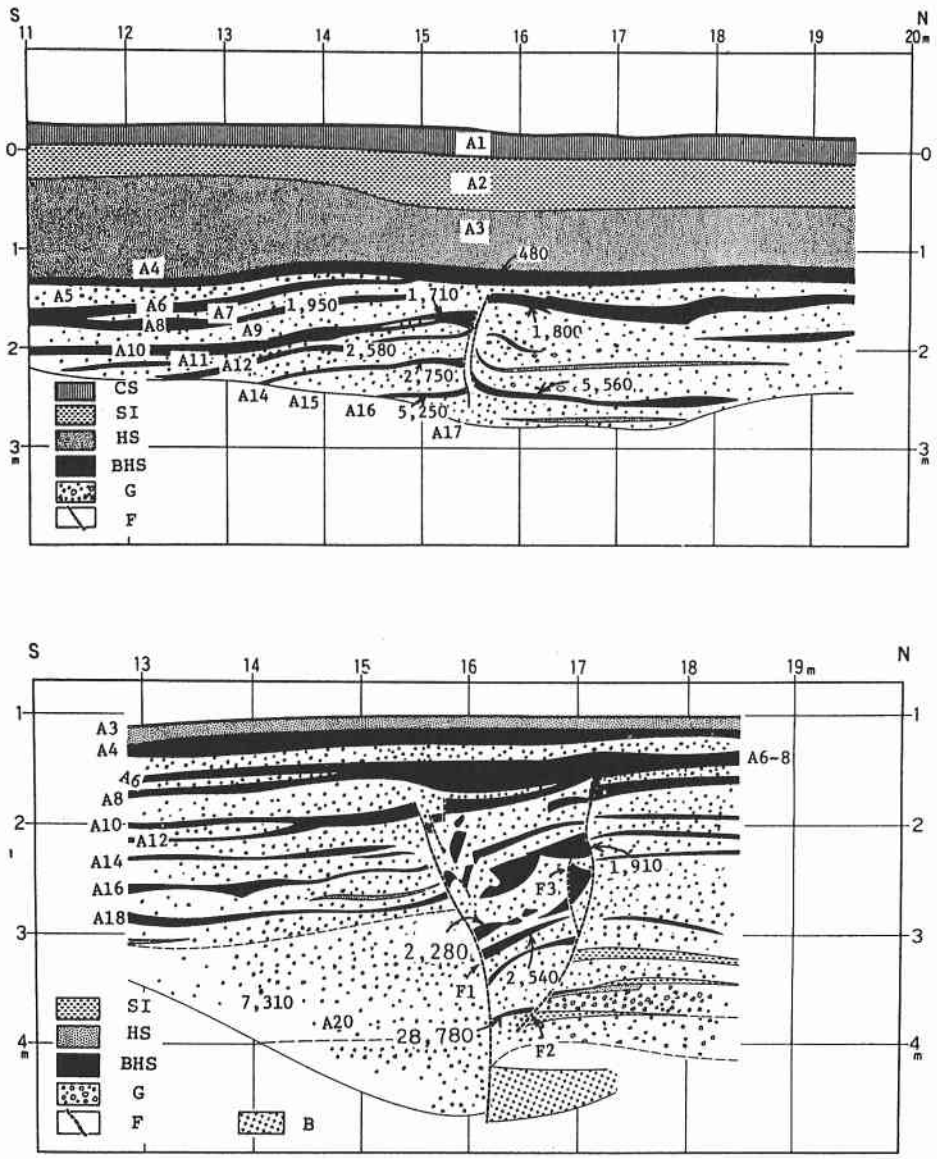

Fig. 6. Geologic section of Trench A, the Yasutomi fault (west wall). B: basement rocks (fault clay or breccia). Other legend is the same as Fig. 3 and 4. Lower: re-excavated exposure (Trench A′ in Table 1).

(Fig. 5). Trench C was located in the next valley about 120 m west of Trench A. The lateral-offsetting feature of the latter valley, its length and width being 460 m and 40 m, was rather gradual. Clear geomorphic features, such as stream offset and fault saddle, at the site of Trench A enabled us to estimate the position of the fault

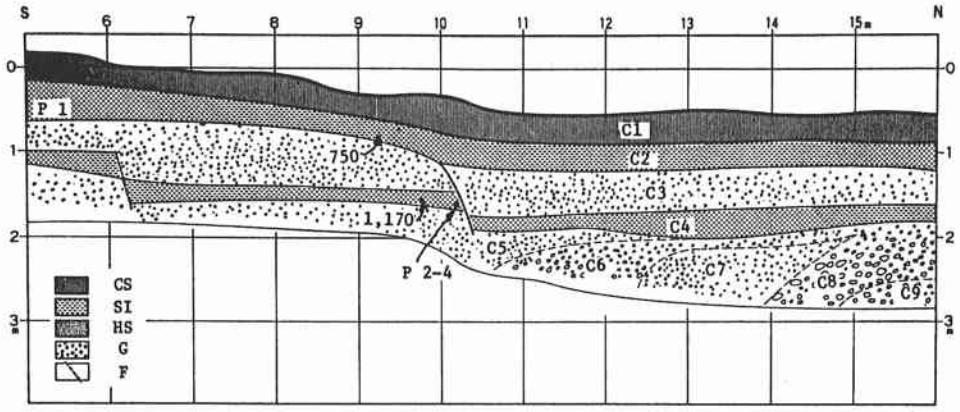

Fig. 7. Geologic section of Trench C, Yasutomi fault. P1 and P2–4 indicate the positions where fragments of earthenwaves were discovered. Other legend is the same as Fig. 3.

trace with an accuracy of 1 m, while the rather vague geomorphic condition in the site of Trench C did not yield exact positioning.

The geologic section of Trench A consists mainly of alternating strata of gravel and black-humic-soil thin-layers, which are cut or disturbed just above the trace of the main fault (Fig. 6). Those disturbed finely grained sediments were covered by horizontally stratified young sediments, indicating the latest rupture. In Trench C, on the other hand, the exposed gravel and humic layers are considerably thick compared with Trench A. The higher sedimentation rate at this site may be due to its higher ability to carry the sediments downstream owing to the greater size of the valley.

^{14}C dating of the humic soil beds revealed that the latest faulting occurred between 480 and 1,800 yrs B.P. at Trench A, and between 750 and 1,170 yrs B.P. at Trench C (Fig. 7). Consequently, the date drops in the range between 750 and 1,170 yrs B.P., or between 780 and 1,200 yrs A.D. This result does not contradict the archeological dating based on the fragments of earthenware buried in the humic soil bed cut by a minor fault in Trench C, showing their dates between the later half of 8th century and 12th century A.D. The fracture of the Yasutomi fault thus confirmed is probably equivalent to the so-called Harima earthquake in 868 A.D. found in a historical document, 'Sandai Jitsuroku', whose discription was so simple that we have not been able to locate its source accurately.

For the purpose of finding events older than the latest one, we re-excavated Trench A up to 5 m in depth (Trench A′, See Fig. 6 and Table 1). The alternating strata were found to be tremendously disturbed below the depth of 2 m in the 1.5-m-wide downpointing wedge-shaped region that converged as going down to the basement rock, that makes up the fracture zone of the main fault. The unconformity of minutely fragmented beds found in the heavily disturbed zone was interpreted as a possible event. The date was determined to be between 1,910 and 2,280 yrs B.P. Because of the extremely complicated geologic section, we could not find more events.

If the above mentioned event is the second latest and periodicity holds, then the

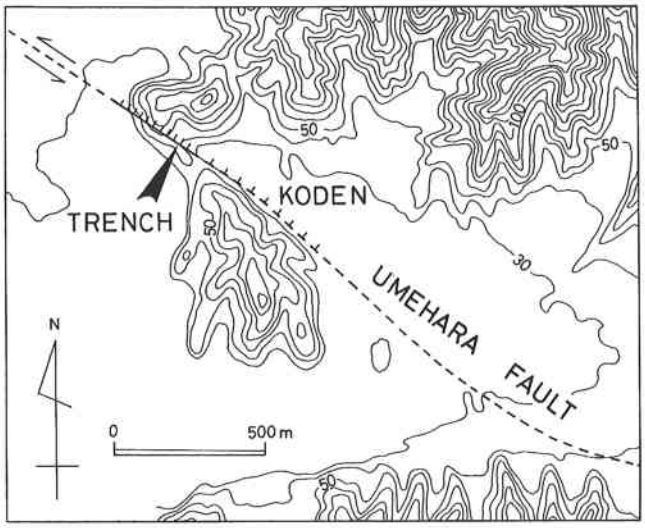

Fig. 8. Topographic map showing the location of the trench at Koden, the Umehara fault, the Nobi fault system. Broken line describes the geomorphologically estimated fault line. The solid line is the part with high certainty.

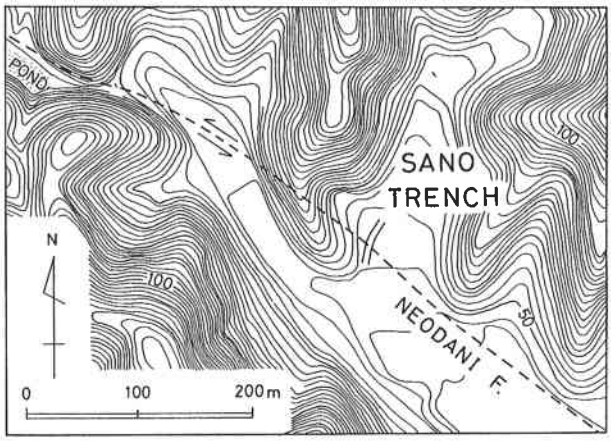

Fig. 9. Topographic map showing the location and the scale of the trench at Sano, southeastern tip of the Neodani fault. Broken line is the estimated fault line.

recurrence interval turns out to be about 1,000 years. Admitting some irregularity, it may well be concluded that the average interval would be within several thousand years.

2.3 Umehara and Neodani faults (Nobi fault system)

Nobi fault system consists of several earthquake faults, namely the Nukumi, Kurot-

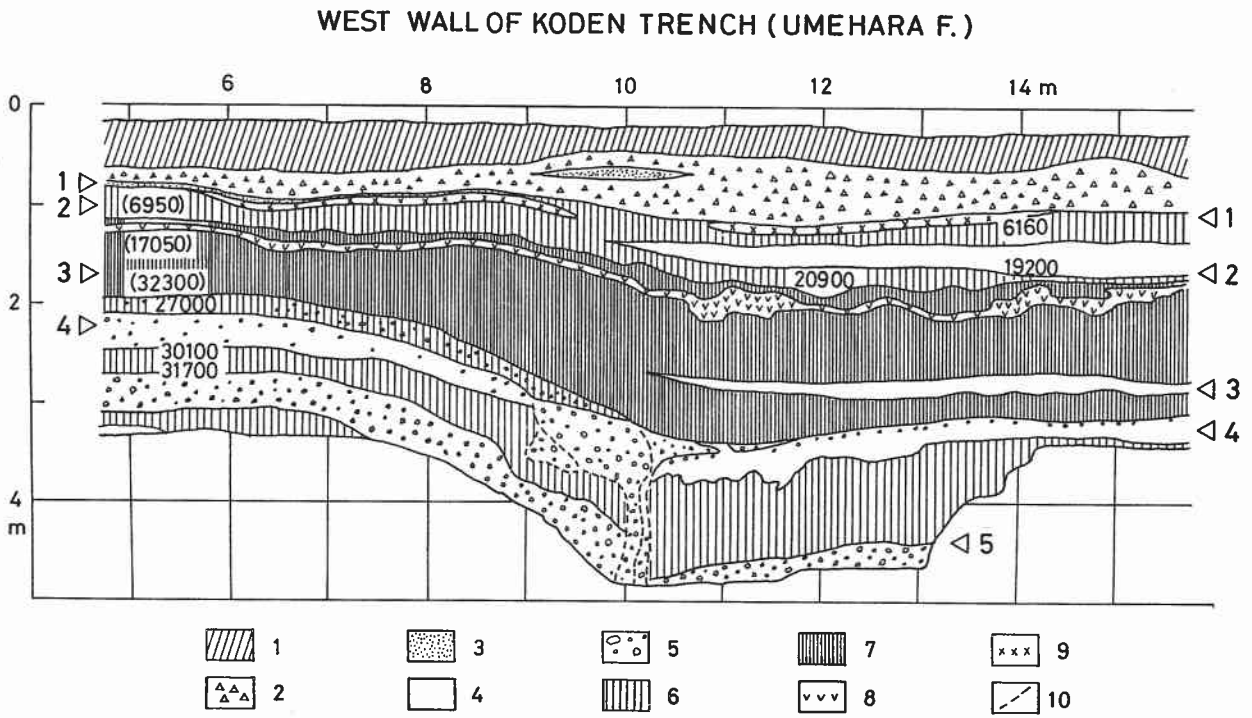

Fig. 10. Geologic section of the Koden trench, the Umehara fault, the Nobi fault system. Numerals indicate ^{14}C dates of the geologic beds in yrs B.P. Parenthesized values, which are preliminary ones, are not adopted in this paper. 1: cultivated soil, 2: gravel (artificial), 3: sand, 4: clay or silt, 5: gravel, 6: humic soil, 7: black humic soil, 8: Aira-Tanzawa ash (volcanic ash), 9: Akahoya ash (volcanic ash), 10: fault.

su, Neodani and Umehara faults (Fig. 2), that ruptured simultaneously on Oct. 28, 1891, giving birth to an M7.9 earthquake, one of the biggest in inland Japan. The selected trenching sites were Koden (Fig. 8), at the central part of the Umehara fault, and Sano (Fig. 9), at the southeastern tip of the Neodani fault. Both sites are about 3 km apart from each other.

At the Koden Trench, strata of culture soil, clay, silt, sand, gravel, humic soil, peat and volcanic ashes had been offset southwestern side up by flexure in the upper part of the geologic section and by a fault in the lower part. The vertical offsets amounted 40 cm at the upper volcanic ash bed, increasing up to 2 m as going down to the bottom of the trench (Fig. 10).

The successive increase of the gap of horizon across the 6-m-wide fault-zone seems to suggest repetitive occurrence of faulting. In order to identify the individual events, we firstly paid attention to clay-silt layers only found on the subsided side of the strata.

It was reported that the 1891 earthquake caused subsidence of the northeastern side of the Umehara fault by up to 1 m. The fresh small basins turned to ponds or marshes by flood after the earthquake. If earthquakes originating from the same fault repeat similarly to the 1891 event, they should be always accompanied by subsidence and flooding. This feature seems to have continued in recent geological ages. In prehistoric ages, the water pool would have been preserved for a long time. Because sedimentation in a pond would be gradual, the possible sediments would be something like clay or silt. The two clay layers that appeared only on the subsided side of the geologic section should indicate the earthquake events; the sedimentation ages of the layers are upper limits of event ages. The events No. 2 and No. 3 in Fig. 10 were

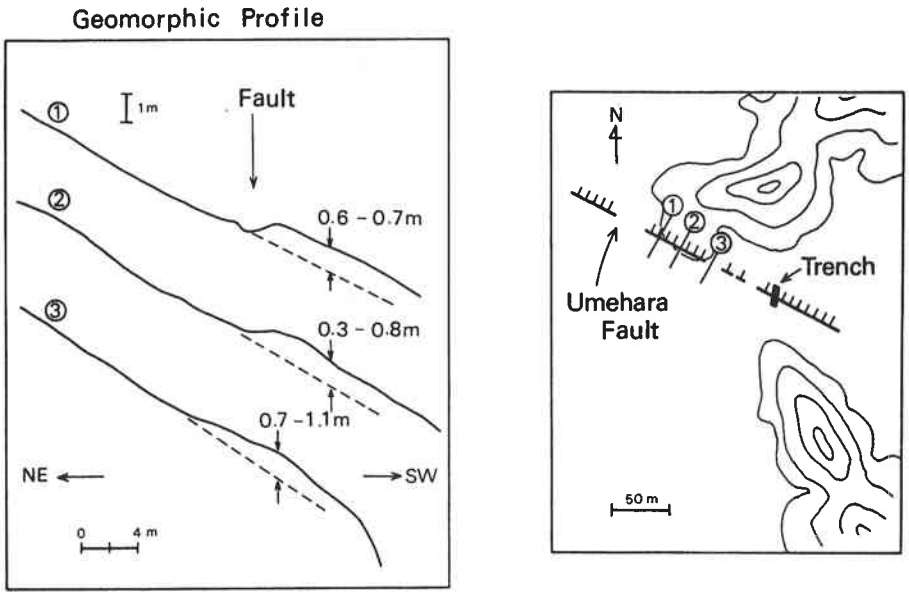

Fig. 11. Geomorphic cross-sections showing surface displacements due to 1891 Nobi earthquake at Koden, the Umehara fault.

thus identified.

In addition to these, three more events were able to be recognized: Event No. 1, the 1891 earthquake, deformed the top humic soil and Akahoya ash layers which were covered by artificial sediments; Event No. 4 and No. 5 made a fault cutting the silt-gravel layer toward the bottom and the bottom gravel layer, respectively.

The offset of a single event amounts to 40 cm, the total being 2 m for five events. This value is in harmony with the surface displacements due to the latest earthquake measured at the nearby fault saddle (Fig. 11).

Dating of strata based on both ^{14}C for humic soil and tephrocronology for volcanic ashes, the Akahoya and the Aira-Tanzawa ashes, constrains the dates of disclosed events. Event No. 2 occurred between 19,200 and 20,900 yrs B.P.; No. 3 between 20,900 and 27,000 yrs B.P.; No. 4 between 27,000 and 30,300 yrs B.P. The fifth event was dated as older than 30,700 yrs B.P.

There is a possibility of an additional event around the time of sedimentation of Aira-Tanzawa volcanic ash, about 22,000 yrs B.P. For, the ash layer had suffered from violent deformation, its thickness greatly changing laterally. It is also conceivable that this ash layer might have be affected by the above mentioned No. 2 event after being buried under the surface. Another possibility is that the disturbance was due to non-seismic gravity instability in the soft sediments. In any way, we have an event or events around 20,000 yrs B.P. as the second latest activity of the Umehara fault. Consequently, the intervals of the long-term activity at the Umehara has not been constant in the recent 30 thousand years, ranging from 5 to 20 thousand years (Fig. 16).

The Sano tench at the Neodani fault did not expose any evidence of faulting in spite of the sufficiently long covering of the geomorphologically estimated fault zone (Fig. 9).

The Neodani fault is believed to be most active among the Nobi earthquake faults. The central portion of the fault has a repeat time of within several thousand years (MATSUDA, 1975). On the other hand, the southeastern tip of the fault is found to have not been ruptured in the recent several tens of thousand years as well as at the time of the 1891 earthquake.

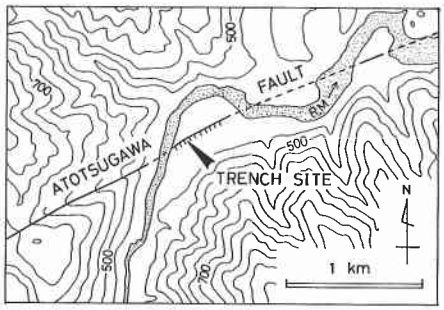

Fig. 12. Topographic map showing the location of the trench at Nokubi, the Atotsugawa fault. R.M. means River Miyagawa.

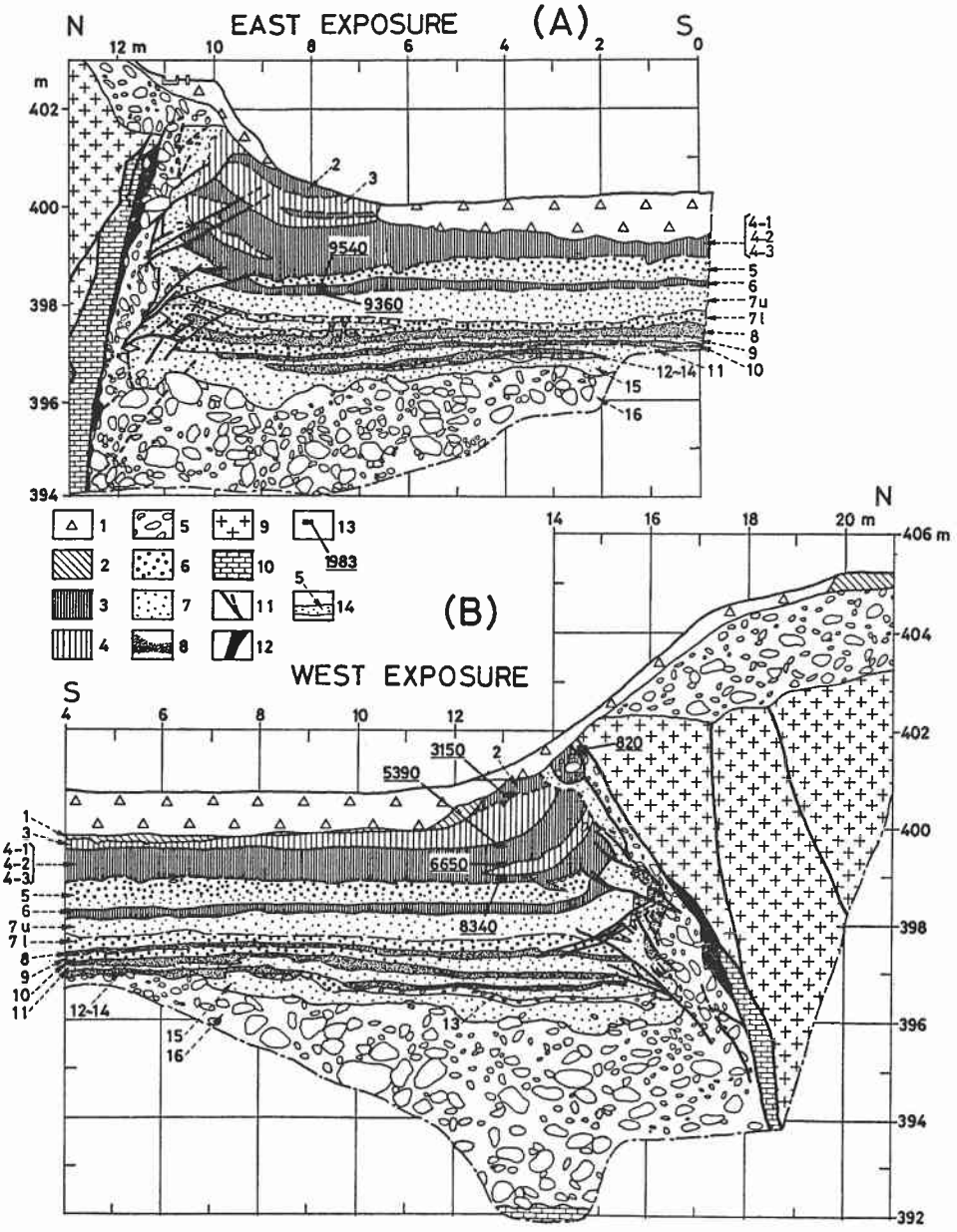

Fig. 13. Geologic section of the east and west walls of the trench, the Atotsugawa fault. The position in the section is given by horizontal distance measured from a reference point at the southern end of the trench and height above sea level. 1: artificial deposit, 2: cultivated soil, 3: humic soil, 4: weak humic soil, 5: gravel, 6: coarse sand, 7: medium sand, 8: fine sand or silt, 9: granite, 10: crystalline limestone, 11: fault, 12: fault clay, 13: sampling position for ^{14}C dating and date in yrs B.P., 14: layer number.

2.4 Atotsugawa fault

A 10-m-deep trench was constructed across the 4-m-high low fault-scarp on the river terrace of the Miya-gawa river, central to western part of the Atotsugawa fault (Fig. 2, 12). Just under the foot of the northern-side-up scarplet, a clear fault plane was exposed (Fig. 13), showing fault movements by striations on the fault clay. It separated granite on the hanging-wall side and yound sediments on the foot-wall side. The strike direction was N70°E, which is in harmony with the trend of the Atotsugawa fault. The dip angle was 65° in the upper part and 75° in the lower part of the trench section.

The accumulated vertical offset was so large at this site that we were not able to correlate the horizons across the fault. So, the uncomformity principle adopted so far in identifying earthquake events was not applicable to the present case.

The sediments in the vicinity of the fault plane were cut by a lot of subsidiary minor faults and deformed to a considerable degree. In the stratigraphic structure, there were weak humic-soild beds in contact with humic soil layers, their thickness diminishing away from the fault scarp (eg., Layer 3 and 4-2 in Fig. 13). Just below the bed, a minor thrust cut the strata. The base of the bed was in unconformable contact with the underlying strata on the upthrown side of the thrust whereas being in conformable contact with those on the downthrown side. We interpreted this structure to be created by slumping of slope deposit at the scarp due to faulting as illustrated in Fig. 14.

The above structures at Layer 3 and Layer 4–2 correspond to Event No. 2 and No. 3,respectively. For Event No. 4 we regarded the gravel found at the bottom of Layer 4–3 as a slumping deposit, making up the key structure with the minor fault that cut the coarse sand (Layer 5) just below it. The latest event (No. 1), on the other hand, was confirmed by the young humic soil of 820 yrs B.P. being cut by the main fault. ^{14}C dates of these events are less than 820 yrs B.P. for Event No.1; 3,150–5,390 yrs B.P. for No. 2; 6,650–8,340 yrs B.P. for No. 3; 8,340–9,540 yrs

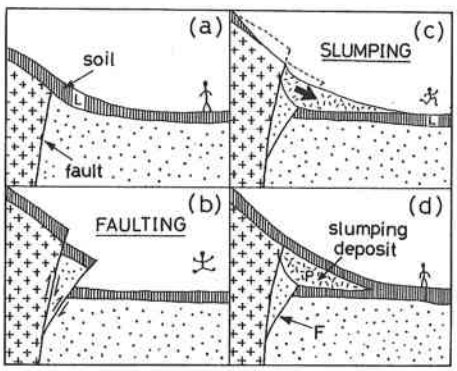

Fig. 14. Key structure for identifying an earthquake event. (a) Before an event: deposition of humic soil layer (L) on the stable slope. (b) Faulting: formation of branching faults. (c) Slumping: formation of slumping deposit layer (weak humic soil). (d) After the event: deposition of soil on the stabilized slope.

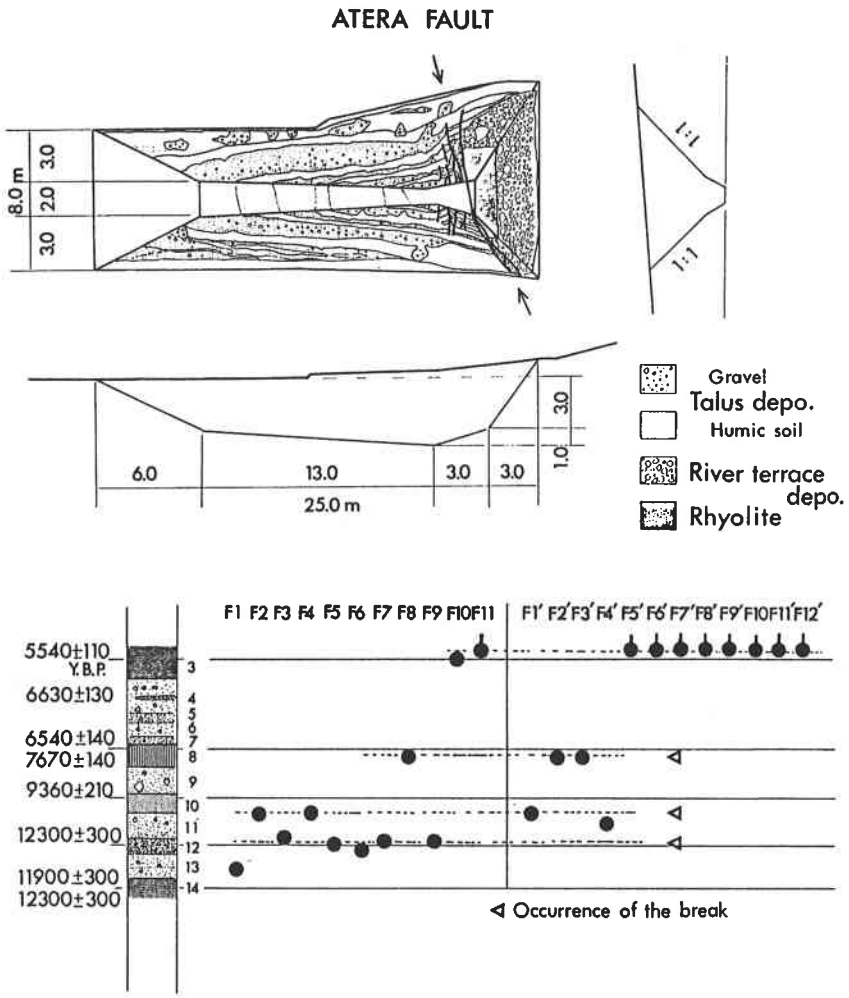

Fig. 15. The trench at Tsukechi, the Atera fault. Upper: outline of the trench. Lower: fault activity of the Atera fault estimated from the occurrence of the minor faults. F1, F2, . . . indicate minor faults. On the vertical axis, ^{14}C dates and layer numbers are shown. Solid circle indicates the break time of the minor fault (after GEOLOGICAL SURVEY OF JAPAN, 1982).

B.P. for No. 4. More events without ^{14}C dating were reported by RESEARCH GROUP FOR EXCAVATION OF THE ATOTSUGAWA FAULT (1983).

Sand and gravel blown up along the fault plane (See Fig. 13) probably indicate the coseismic liquefaction of soft sediments. The date of the latest mechanical disturbance was obtained by measuring the magnetic vector of the sand in reference to the geomagnetic secular variation based on the magnetism of baked clay at the old kilns and hearths excavated in the Kinki district (HIROOKA, 1971; SAKAI and HIROOKA, 1983). This archeomagnetic study shows that the date falls on either 80±20 A.D.

or 1,880±60 A.D. Since the former solution contradicts with the C date of the latest event, we should adopt the latter. The determined date coincides well with that of the historical earthquake of 1858, the so-called Hida earthquake.

An outcrop study at the eastern end of the Atotsugawa fault, and the finding a piece of buried wood dated at 490 yrs B.P. at the exposed fault, also suggests that the Hida earthquake was nothing but the ruture of the greater part of that fault (TAKEMURA, 1983; TAKEMURA and FUJII, 1983).

2.5 Atera fault

The Geological Survey of Japan conducted the trenching study at Tsukechi, the central part of the Atera fault (Fig. 2). The trench was across the 3-m-high northeastern-side-up fault scarp (Fig. 15).

A horizon cut by subsidiary minor faults was a key to the identification of an event. The more the minor faults are concentrated on some horizon, the higher is the possibility of the earthquake occurrence around the age corresponding to the horizon (GEOLOGICAL SURVEY OF JAPAN, 1982).

The upper section of the trench was artificially disturbed, so that the latest event seems to be missing. Four events were identified and dated by ^{14}C. The possible second latest was dated less than 5,540 yrs B.P., with others being once between 6,540 and 7,670, and twice between 9,360 and 12,300 yrs B.P., respectively.

Meanwhile, HIRANO and NAKATA (1981) studied an outcrop, several kilometers northwest of the above mentioned trenching site along the Atera fault (Fig. 2). The exposure showed appreciably disturbed alternating strata of gravel and humic-soil together with main and subsidiary faults. Upper cutoff of the humic-soil layers by gravel layers was interpreted as evidence of an earthquake. Estimated four events have dates of 1,850, 5,500, 7,900 and before 10,300 yrs B.P. These fall well within the ranges obtained by trenching at Tsukechi. According to the above estimation, the latest event occurred around 100 A.D., which is rather old compared with the historical earthquake of 762 A.D., a candidate for a large earthquake that ruptured the Atera fault (OKADA, 1975).

Another study on a fault outcrop was made by OKADA and MATSUDA (1976) at the southeastern part of the fault. Their result shows that the date of the latest event should be less than 4,300 yrs B.P., and that large earthquakes occurred with a repeat time of 2,000–4,000 years as suggested by alternating accumulation of sand-gravel beds and black soil layers on the downthrown side in a 2,000–4,000 year interval. Their conclusion has no contradiction with the result of the trenching.

3. Microseismicity as Medium-Term Activity

Generally, seismicity is high in the highly populated regions of active faults, such as the Kinki and Chubu districts, and is low in the scanty regions, such as the central part of Chugoku district, some parts of Shikoku and southern Kinki (Fig. 1). However, it is not true that all of the active faults are seismically active. Some active faults are unaccompanied by concentrated foci along them. Among them, the Atera fault and Median Tectonic Line are typical examples. Moreover, the degree of concentra-

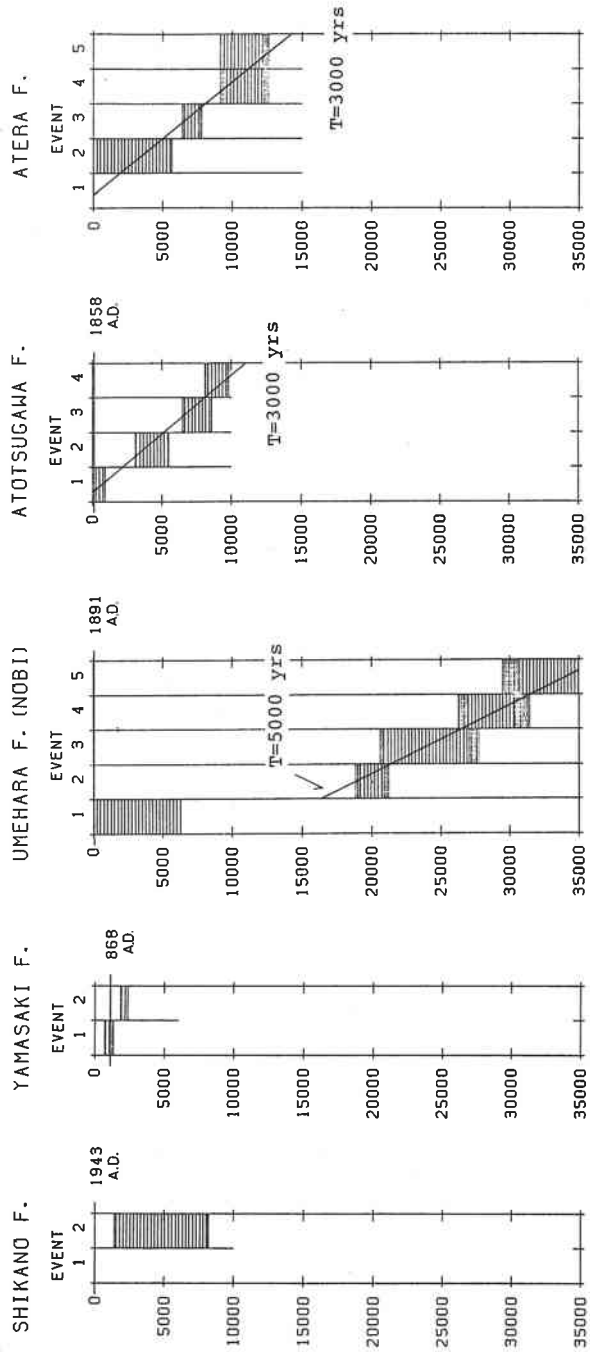

Fig. 16. Estimated range of occurrence time versus earthquake event number for each fault. The upper and lower limits of the time are defined to be the dates of the horizons nearest to the corresponding event subtracted or added by measuring errors, respectively. The error range is shown by rather black shadow. Lower interruption of columns indicates the termination of datable geologic beds. For the Shikano and Yamasaki faults, the results of different trenches are summarized into reduced one taking common extents of the ranges of occurrence times. Historical earthquakes are indicated by horizontal bars with their dates in years A.D. Average recurrence intervals for individual faults are obtained by fitting a straight line so as to pass through the shaded zone. 5,000 years for the Umehara fault before 20,000 years; 3,000 years for both the Atotsugawa and Atera faults.

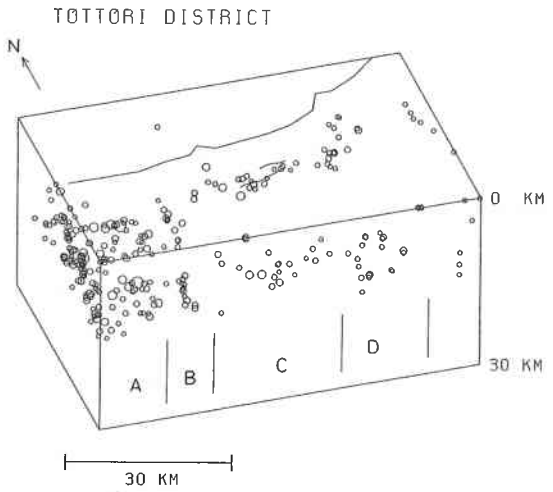

Fig. 17. Microearthquake distribution around the Shikano and Yoshioka faults. Foci with magnitude 1.5 or more during the period from Apr. 24, 1976 to Dec. 31, 1981 are projected on a horizontal plane and vertical planes in both N–S and E–W directions. The diameter of the circle indicating a hypocenter is increased with its magnitude. The sections A, B, C and D represent separated groups of foci.

tion of microearthquakes on a fault differs from fault to fault. The Atotsugawa fault has fairly concentrated foci along the 70-km-long nearly straight fault-line.

The difference in seismicity around active faults may partly arise from local stresses and properties of medium, and also have a close relation to a certain stage in a long-term activity cycle. In the following, microearthquake distribution on and around some typical active faults will be reviewed.

3.1 Shikano and Yoshioka faults

The 1943 Tottori earthquake (M7.4) caused right-lateral slips along the Shikano and Yoshioka faults, which run nearly parallel 2 km apart. Microearthquakes along these faults and their bilateral extensions are considered to be aftershocks in the broad sense of the most recent large earthquake. Figure 17 shows the three dimensional distribution of foci around the faults. The distribution is partitioned in four sections (A, B, C and D) divided by clear seismicity gaps. Section C covers the two faults. The foci fairly concentrate on the Shikano fault. The fault structure estimated by microseismicity is such that the fault system, the Shikano and Yoshioka faults, is 25 km long and 8–10 km deep shallowing toward the both ends.

The aftershocks just after the M7.4 earthquake were also distributed beyond Section C, the majority taking place in the west sections A and B (JAPAN METEOROLOGICAL AGENCY, 1982; OMOTE, 1955). Microearthquakes in Section B have a north-south linear trend nearly perpendicular to that of the Shikano fault, suggesting 10-km-long latent vertical fault or fracture zone other than the Shikano and Yoshioka faults. We used the term "fracture zone", here, against a group of subsidiary latent

faults estimated by microearthquakes. The medium-scale M6.2 earthquake of Oct. 31, 1983 occurred almost at the fracture zone of section B (TTOTTORI MICROEARTHQUAKE OBSERVATORY AND MICROEARTHQUAKE RESEARCH SECTION, DISASTER PREVENTION RESEARCH INSTITUTE, KYOTO UNIVERSITY, AND INSTITUTE OF EARTH SCIENCES, TOTTORI UNIVERSITY, 1983). Its aftershock area was 10 km long extending in an NW–SE direction. Aftershocks in the early stage had a trend of NWN–SES direction at the northern part of the area. The focal mech anism of the main shock shows nearly pure strike-slip faulting, one of the fault planes running in an NW–SE direction. These features are in harmony with the estimated latent fracture zone.

The foreshocks of the M7.4 earthquake, including M6.1 and M6.4 events, took place around section D, according to the result of relocation of hypocenters (JAPAN METEOROLOGICAL AAGENCY, 1982). This activity, about a half year before the main shock, may possibly be related to another latent fracture zone.

In this case, we have subsidiary medium-term seismic-activities originating from the subsidiary latent faults before and after the long-term main activity of the Shikano and Yoshioka faults. The aftershock activity on the Shikano fault, Section C, is relatively low compared with the other sections. The large slip on the fault might have resulted in effective release of the accumulated stresses around the fault.

3.2 Atotsugawa fault

As evidenced by the trenching study, the most recent large earthquake at the Atotsugawa fault occurred about 120 years ago. The elapsed time from the event is about three times longer than that of the Shikano fault. This fault provides microseismicity of another different stage of earthquake cycle.

Outstanding alignment of foci can be traced over 70 km along the Atotsugawa fault as well as over 10 km along the eastern part of the Mozumi fault (Figs. 2 and 18), which is not found in other regions in Fig. 1. Both ends of the Atotsugawa fault have relatively shallow foci, suggesting the termination of the fault.

The activity concentrated on the fault plane may be caused by non-uniform faulting along the entire fault during the latest large earthquake. The heterogeneous distribution of foci may reflect this nature. The low seismic region, Section B in Fig. 18, should be the place where the stresses were almost completely released by the historical earthquake. Section A includes several seismic spots and gaps. Relatively small magnitude of 6.9 estimated by the earthquake damages (USAMI, 1975) as for a long fault of 70 km could be explained by the idea that the slipped area was restricted to some patches leaving a large amount of unbroken area, or barriers (AKI, 1984), where stresses have been concentrated up until now generating microearthquake (MIKUMO and WADA, 1983; TSUKUDA, 1983).

3.3 Yamasaki fualt

The result of the trenching study combined with a historical document shows that the latest large earthquake took place along the Yasutomi fault, the eastern segment of the Yamasaki fault. The elapsed time up to now is about 1,100 years.

In contrast to the Shikano and Atotsugawa faults, the microseismic distribution is rather widely spread in both sides of the fault without concentrating on the fault

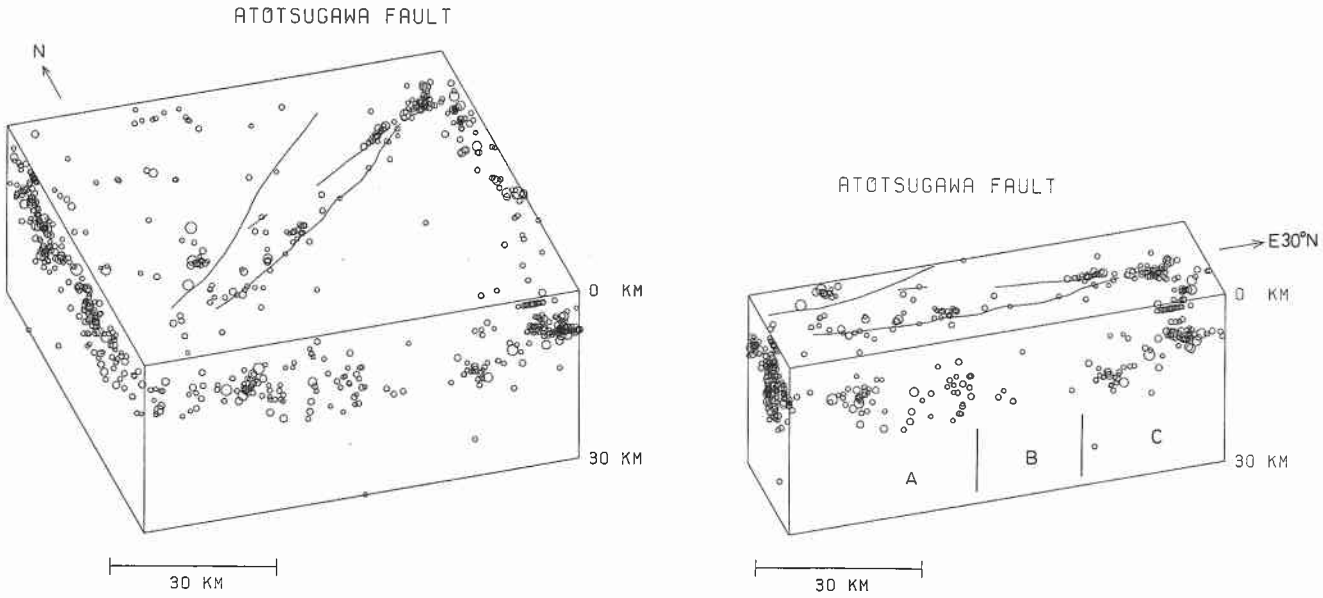

Fig. 18. Microearthquake distribution around the Atotsugawa fault. The period is from Jun. 1, 1977 to Apr. 30, 1979. Magnitude range and the way of projection are the same as Fig. 17. The right shows the concentrated distribution along the Atotsugawa fault. A, B and C denote regions along the fault.

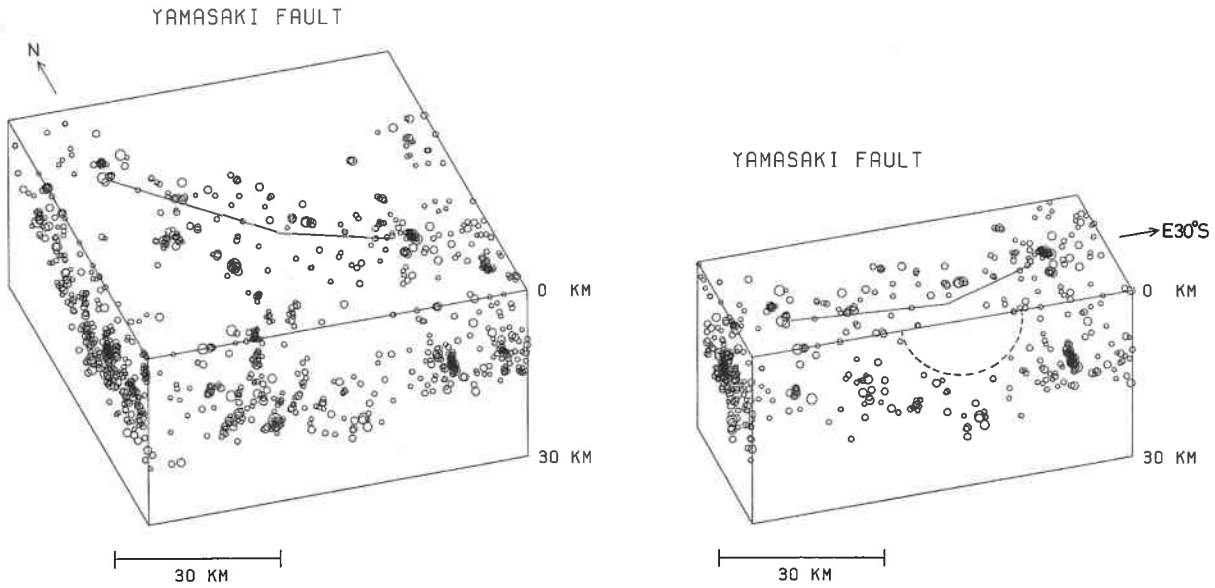

Fig. 19. Microearthquake distribution around the Yamasaki fault. Magnitude range, the period and the way of projection are the same as Fig. 17. The right shows the distribution just beneath the fault trace. The region surrounded by broken line is an aseismic part of the fault plane.

plane, probably due to the sufficiently long lapse of time to relax the post-seismic stress concentration along the fault (Fig. 19). However, studies on structures of clustering foci have revealed that some clusters, as small as less than 1 km in diameter, have a linear trend parallel to the strike of the Yamasaki fault (TSUKUDA, 1978; NISHIGAMI and TSUKUDA, 1982). These evidences suggest the existence of fracturing planes along the main fault. The 20-km-wide seismic zone along the fault may characterize some later stage of fault activity in a seismic cycle.

Subsurface structure of the fault zone is such that the 20-km-wide and 10-km-deep aseismic area are surrounded by clustering foci, which are deep at the center and shallow towards the both ends (Fig. 19). The aseismic area may correspond to the source region of the last large earthquake.

4. Microseismicity as Short-Term Activity

We will show the temporal change of the degree of microseismic activity around the Yamasaki fault. To evaluate the activity we will use newly defined parameters.

4.1 Definition of seismic activity and extended b value

The total number, N, of earthquake observed during a certain period and in the region concerned is given by

$$N = \int_{M_0}^{\infty} n(M)\ \mathrm{d}M \tag{1}$$

where $n(M)$ is number density of earthquakes as a function of magnitude M, and M_0 is the minimum magnitude concerned. It is reasonable to define the activity A in such an integral form as

$$A = \int_{M_0}^{\infty} w(M)\ n(M)\ \mathrm{d}M \tag{2}$$

where we assume the activity is characterized by only magnitude and the number density. $w(M)$ acts as a weight function for magnitude. The integrand $a = w(M)n(M)$ means activity density.

When we adopt such weight function as $w(M) = 1$, the activity is namely the total number. The other extreme case is such that the weight is the seismic energy corresponding to a given magnitude. Then the total released seismic energy is a measure of seismic activity. The former formula deals with all events having an equal weight so that the samll ones with a large number would become predominant. On the other hand, the latter makes only large events significant.

To mediate above extremes, another definition of the weight function is proposed as follows:

$$w(M) = \exp\ (b_0'\ (M - M_0)) \tag{3}$$

where $b_0' = b_0 \ln 10$, and b_0 is the minimum b value that should be estimated beforehand.

The above formulation comes from the idea that an earthquake source, which

occupies some area of a plane generated by faulting, is considered to be composed of small parts of the fault plane. In other words, an event is regarded as a summation of small events. We measure the degree of activity by the total area obtained by integrating the areas of inidivual faults. The probability of an earthquake to grow to some magnitude seems to follow such an exponential law as the Gutenberg-Richter's formula. If the probability is inversely proportional to the fault area, the Gutenberg-Richter's b value would be nearly equal to 1, where an empirical relation between magnitude and fault size is used (KANAMORI and ANDERSON, 1975). In this case, the activity is proportional to the integrated area of faults. Actually the b value is scattered temporarily and from region to region, the minimum value being around 0.7 in our data described later. Then, the weight funcion here has merely the meaning the normalizing the magnitude frequency by the probability of occurrence of the magnitude. In any way, the activity defined here is approximately proportional to the area of the total fault surface produced by earthquakes.

If we adopt the weight function (3) and if the number density takes the Gutenberg-Richter's formula, namely,

$$n(M) = \exp\ (-b'(M - M_0)) \tag{4}$$

where $b' = b \ln 10$, and b denotes b value. In this case, b value is simply derived by

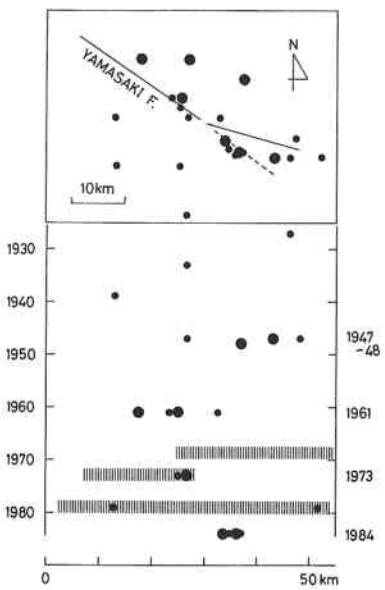

Fig. 20. Space-time pattern of recent major earthquakes around the Yamasaki fault. The epicenters are projected on the E-W axis. Large solid circle: $5 \leq M < 6$. Small one: $4 \leq M < 5$. Data source is the earthquake list of Japan Meteorological Agency. Shadow means high microseismic activity. The 1984 earthquake of $M5.6$ is added after submission of this paper.

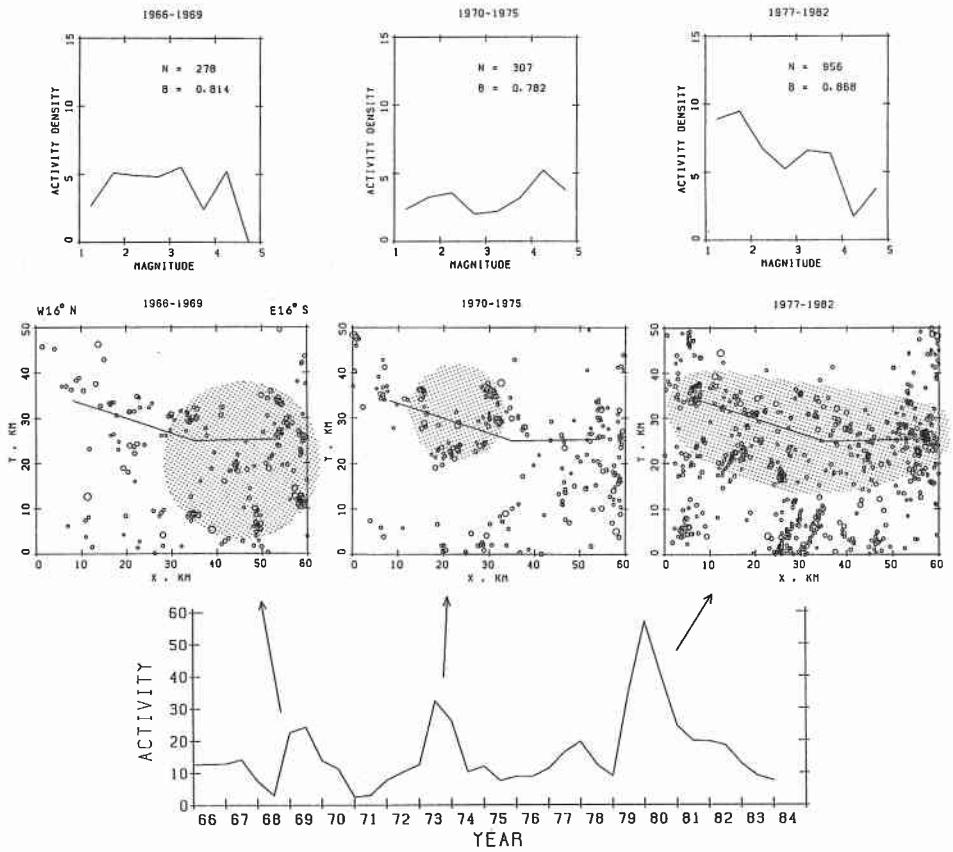

Fig. 21. Temporal variation of seismic activity and distribution pattern around the Yamasaki fault from 1966 to 1983. Middle: epicentral distributions for different periods corresponding to activity peaks. Bottom: seismic activity defined in the text for the region shown on the middle; The values are plotted at a half-year interval, being calculated for one-year period centering on the plotted times. Top: activity density for each period together with b values (extended b value given in the text); N, B denote the total number of earthquakes and b value, respectively.

$$b = b_0 A/(A-N). \tag{5}$$

That calculation is valid only if $b_0 < b$. This is one of reasons why we use the minimum b value as b in the function (3).

Equation (5) is considered to be an extented definition of b value. This formula gives a value similar to b value even when the frequency distribution does not obey the Gutenberg-Richter's law.

4.2 Temporal variation of microseismicity around the Yamasaki fault system

In recent 60 years, seismic activity around the Yamasaki fault became particularly

active in 1961, when a swarm-like activity with the largest event of magnitude 5.9 occurred at the central part of the fault system, the southeastern tip of the Hijima fault (Figs. 2 and 20). Since, then, a 4-year-period recurrence in activity has been observed as pointed out by OIKE (1977). The activity peakes appeared in the years of 1965, 1969, 1973, 1977, and 1979–1980 (Fig. 21).

The seismic activity defined above is used here, normalized by both time and space taking the units as 1 year and 100 km, respectively. The minimum magnitude, determined by the capability of detection by the observation network, is 1.0, and minimum b value, slightly lower than the empirical minimum value, is assigned to be 0.675. Activity A, then, means that the expected number of events with magnitude 1.0 would be A during a year and in a region of 100 km^2, if all the events are decomposed into the smallest ones.

The microseismicity, routinely monitored since June 1965, shows that the activity has been changing with peaks and troughs. Quiescent periods precede peak activities. The recurrence time of peaks is 3–4 years. The duration of each highly active period is about 2 years if we take the pulse width at a half height of the pulse. The extended b value is, for the most part, inversely correlated to the activity. However, it maintained a constant level for some periods. b value seems to be closely related to the extent of the relevant seismic regions as suggested in what follows.

The 18-year-period microseismicity is roughly divided into three stages in reference to the change of the spatial pattern of seismicity (Fig. 21). In the first stage, with a 4-year period duration, the active region with clustering spots was biased to around the eastern part of the fault system. It should be noted that the spots encircle the fault segment instead of concentrating on the fault. The previously defined activity density in this period has a relatively flat characteristic against magnitude with a b-value of 0.81 (Fig. 21).

In the second stage, during the next 6 years, the clusters moved to around the western segment of the fault system. The active area is smaller than that of the former stage by about a half in linear dimension. The b value dropped to 0.78, which is low compared with other periods.

In the last stage, the last 6 years, the whole area became active with a high b value of 0.87. It is noteworthy that the clusters with high activity appeared at the both ends of the fault and around the southern margin of the seismic zone, and that several small clustering spots were distributed surrounding the fault. The b values for the above different seismic patterns suggest that a low value may occur for a small seismic area, whereas a high value corresponding to a somewhat dispersed seismic area.

5. Discussion

The purpose of our trenching was to make clear the long-term large earthquake sequences for individual active faults distributed adjacently and to see whether any correlation exists among them. In parallel with this paleoseismic study, we have studied the medium- to short-term fault activity in terms of microseismicity. Although the data obtained so far are not sufficient to present a consistent model to explain the

whole range of an earthquake cycle, particularly for the medium-term ragne, we will discuss some problems concerned with the activity of intra-plate active faults in southwest Japan.

The horizontal strain rate there measured by triangulation amounts up to about 2×10^{-7}/year, the maximum principal axis striking SE–NW or E–W (NAKANE, 1973). If this rate has maintained through geological ages, then the highest rate of generating earthquakes of $M7$ or greater in certain region should be once in a few thaousand years, because the associated strain-drop is considered to be of the order of 10^{-4}. The Yamasaki, Atotsugawa, and Atera faults have the highest activity rates, estimated recurrence times being 1,000, 3,000 and 3,000 years, respectively (Fig. 16). Active faults in southwest Japan, mostly strike-slip faults, make a role to lower the increasing horizontal crustal strain by generating earthquakes.

The representative faults including the above faults are about 70 km long for each. The postseismic increase of local strain, particularly around the both tips of the fault, may cause considerable imbalance of the stress field around the fault, affecting the associated subsidiary faults as well as neighboring major faults.

The Atotsugawa and Atera faults, a dextral and sinistral fault pair, seem to form a large-scale mechanical conjugate system in central Japan under the E–W trending horizontally compressing stress field (HUZITA *et al.*, 1973). It is interesting to see whether the pair has ruptured at the same rate to compensate for the unbalanced local stresses. Trenching results support the above property, for the average recurrence times of the two faults were almost the same, and nearly contemporaneous activities of the pair were found (Fig. 16).

The Nobi fault system is more than 70 km long in linear dimension. It is composed of mainly several strand faults of 40 km length or less. According to the study of the strong motion seimograms by MIKUMO and ANDO (1975), the 1891 Nobi earthquake initiated at around the Nukumi fault, the northwestern end of the system, propagating southeastwards from fault to fault to stop at around the Umehara fault, the other end of the system. This case was a typical example of strong coupling of nearby parallel faults. The stress concentration at the tip of a fractured fault triggered the fracturing of the next fault, and so on. Furthermore, the rupture process was not simple even on a single fault. Bending of the fault line along the Neodani fault, the principal fault of the system, generated anomalous horizontal displacement field at the kink of the fault, producing local large vertical offset of 6 m which is comparable to the maximum horizontal slip of 8 m (MATSUDA, 1974). Such an unstable successive faulting is not always the case as confirmed by the trenching study. The Umehara fault had a long quiescent period of 20,000 years before the great Nobi earthquake, whereas the central part of the Neodani fault is believed to be more active (MATSUDA, 1975).

The trenching of the Umehara fault provided a definite example of irregular intervals of faulting. The recurrence time was about 5,000 years from 20,000 to 30,000 yrs B.P., and 20,000 years after that period. It seems to be quite reasonable that the densely populated intraplate active faults does not have a constant rate of activity, particularly for a set of faults distributed adjacently in parallel, because the effective release of accumulated strain in a region would not always need fracturing of all

the faults there. So that, the so-called time predictable model (SHIMAZAKI and NAKATA, 1980) does not seem to be applicable to intraplate faults. This model is based on the data from interplate faulting where the upper limit of the amount of accumulated strain around a segment of a boundary fault is directly related to the magnitude of its faulting, the characteristic earthquake of the segment.

The small active fualts, including subsurface latent fualts, around the edge of a master fault have a role of decreasing anomalous stress field produced by a large slip on the master fault. The Shikano and Yoshioka faults, which have a 20-km-long microseismic region are accompanied by subsidiary latent faults, as estimated by microearthquake distribution, that extend the seismic area over 50 km bilaterally. The majority of the foreshocks and aftershocks of the 1943 Tottori earthquake (M7.4) took place on such faults or their neighborhood. The 1983 earthquake of M6.2 had a conjugate fault plane with the Shikano and Yoshioka faults, adjusting unbalanced stress field around the western terminal of those two faults. The aftershock activity has been particularly active in the region of western latent faults compared to the main faults, lasting for more than 40 years.

Similarly, the Nobi fault system has a latent fault confirmed by levelling and triangulation before and after the great Nobi earthquake (MIKUMO and ANDO, 1975). The fault is situated at the southeastward extension of the Neodani fault. The 1891 rupture, propagated southeastwards, branched off into the two faults, the Umehara fault and the above latent fault. A noticeable group of microearthquakes, presumably aftershocks of the event of about 90 years ago, are seen around the southeastern end of the system, between the Umehara fault and the latent fault (Fig. 1, 2). The rather dispersed distribution may suggest that there are more small subsurface faults. However, the major faults of the system have a rather low microseismicity along them.

As ascertained by the above two cases, the Tottori and Nobi earthquakes, the most slipped parts of the earthquake faults would form a low seismic area in aftershock activity. The Atotsugawa fault has a 20-km-long remarkable aseismic segment, probably corresponding to the center of the 1858 earthquake of M6.9. The aftershocks of the event have continued for more than 120 years just along the fault, mainly on the western tip of 30 km and the eastern tip of 20 km.

The Yamasaki fault has a similar aseismic area on the eastern segment, the source of the historical earthquake of M7.1 about 11,000 years ago. This implies that the slipping center of a fault will remain aseismic for a long time, probably until the next large earthquake. The above nature supports the concept that a fault or its segment has recurrent earthquakes, whose magnitudes are characterized by the size of the fault or its segment, and that the frequency of smaller earthquakes is often lower than expected by the Gutenberg-Richter's law (WESNOUSKY *et al.*, 1983; SCHWARTZ and COPPERSMITH, 1984).

We have looked at so far two types of aftershocks: the first is an on-the-plane type, where the earthquakes concentrate on the fault plane, as observed along the Atotsugawa fault; and the other a branching type, where the shocks are distributed around subsidiary faults branched off from the edge of the main fault, as noticed in the Nobi fault system. In the Shikano fault region, we have both of these. These types of microseismicity, however, have not been found in the Yamasaki fault region.

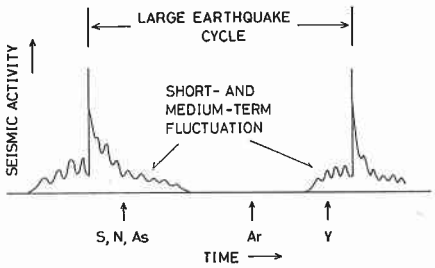

Fig. 22. Schematic seismic-activity variation for a large earthquake cycle. S, N, A_s, A_r, and Y denote the Shikano, Nobi, Atotsugawa, Atera and Yamasaki faults, respectively.

The Yamasaki fault is probably in a post-aftershock stage of the latest large earthquake, and possibly in a pre-seismic stage of the next event.

Another case of typical microseismic pattern is seen around the Atera fault. Although the fault is one of the highest active faults in Japan as revealed by a trenching atudy (GEOLOGICAL SURVEY OF JAPAN, 1982) and a geomorphic study (SUGIMURA and MATSUDA, 1966), the 70-km-long and 20-km-wide region covering the entire fault is extremely low seismic (Fig. 1). The region outside the aseismic area has a considerable seismic activity. If we assume that the latest large earthquake occurred one or two thousand years ago, though the date has not been definitely confirmed yet, then the present aseismic state indicates a mid stage of the inter-seismic interval of 3,000 years.

As discussed above, the different pattern of the present microseismicity from fault to fault is easy to relate the lapse time from the latest main event. We have three groups of faults: the first is in an "aftershock" stage; the second in a mid stage; and the third a "foreshock" stage. The Shikano, Atotsugawa, and Nobi faults are considered to belong to the first group. The Atera and Yamasaki faults are probably classified into the second and third groups, respectively (Fig. 22).

Recurrence times of long-term large earthquake activity are 1,000 years or more (up to 5,000 years) for the Yamasaki fault, about $3,000 \pm 1,000$ years for the Atotsugawa and Atera faults, 4,000–8,000 years for the Shikano fault, and 5,000–20,000 years for the Umehara fault (Fig. 16). Three to four year period recurrence is found in the microseismicity in the Yamasaki fault region owing to relatively long-lasting observation of about 20 years. We regard this periodicity as a short-term characteristic. Almost the same recurrence time is found in the region of the Shikano and Yoshioka faults (TSUKUDA *et al.*, 1976). In the Atotsugawa fault region, a 2 year period fluctuation is found during the recent 5 years (TSUKUDA, 1983).

On the other hand, the data to find recurrence times of the medium-term activity are quite limited. The Yamasaki fault provides us with a valuable example. As seen from Fig. 20, activity with magnitude 5–6 occurred 4 times in the recent 50 years with a period of 11–13 years. Activity with magnitude 5.5 or more recurred once at an interval of 23 years. Such medium-scale earthquakes represent the medium-term activity.

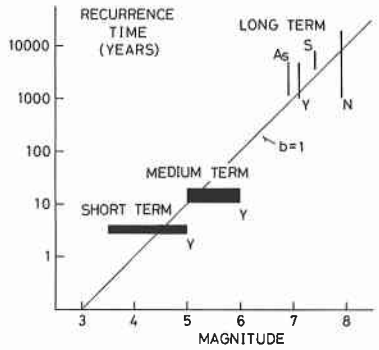

Fig. 23. Recurrence interval versus earthquake magnitude. Y, A_S, S, and N denote the Yamasaki, Atotsugawa, Shikano and Nobi faults, respectively. The magnitude of the characteristic earthquake in the long-term activity is assumed to be that of the latest large earthquake associated with the relevant fault.

Figure 23 shows the summary of the recurrence times for short-, medium- and long-term seismicity. The activity of Nobi fault system is evaluated by taking account of both the high activity of the Neodani fault with a recurrence time of about 1,000 years and the relatively low activity of the Umehara fault. Although the individual faults belonging to the fault system must have characteristic earthquakes smaller than the 1891 earthquake, the plot for the Nobi fault system in the figure marks the magnitude 7.9 of the event. The medium-scale earthquakes in the Yamasaki fault region show slightly higher activity rate than expected by the Gutenberg-Richter's law with a b value of 1 or so. This unusual activity may support that the fault is in the stage before the forthcoming large earthquake.

6. Conclusion

Long-term recurrence times of large earthquakes in southwest Japan disclosed by trenching of active faults are as follow: 1,000 years or so (less than 5,000 years) for the Yamasaki fault in the western Kinki district; about 3,000 years for the large-scale conjugate pair, the Atotsugawa and Atera faults in the central Japan; about 6,000 years for the Shikano fault in the eastern Chugoku district; about 5,000 years before 20,000 yrs B.P. and 20,000 years for the last cycle for the Umehara fault (Nobi fault system) in the Chubu district. Medium-term recurrence time of smaller earthquakes of $M5$–6 is 10 to 20 years for the Yamasaki fault. Short-term recurrence time found in the microseismicity around the Yamasaki fault is 3–4 years.

Trenching method proved its validity on the points of precise location of historical earthquakes and determination of sequential earthquake events. The method of identification of events should have been changed from fault to fault because of different geologic circumstances.

Because that medium- and short-term activities involve more than one event, it

is necessary for us to evaluate seismic activity integrating the contributions of individual events. Newly introduced quantity measuring the degree of seismic activity is nearly in proportion to the total fractured area produced by earthquakes. The activity density with respect to magnitude and extended b value are useful for describing the differences of magnitude distribution of seismicity.

Present microseismicity around an active fault reflects the latest large earthquake and the elapsed time from it. Large aseismic domain on the fault plane as found for the Yamasaki and Atotsugawa faults is probably the source of the event. The outstanding feature of concentrated microearthquakes on the Atotsugawa fault inform us of the relaxation process of stress concentration due to the last large earthquake. Recent microseismicity around the Yamasaki fault shows peculiar temporal and spatial properties. There is a possibility that this indicates a precursory activity of the next large earthquake.

The author is much indebted to his many co-workers in trenching of active faults. Among them, Dr. M. Ando, who first drew up the plan for trenching in Japan, and Dr. A. Okada, our chief leader, should be greatly acknowledged. The research group for trenching of the Nobi fault system in 1981 includes A. Okada, M. Ando, T. Tsukuda, M. Watanabe, K. Okumura, Y. Takehana, T. Nakata, S. Hirano, and others. The members in 1982 for the Atotsugawa fault are A. Okada, T. Tsukuda, Y. Ikeda, A. Takeuchi, T. Takemura, M. Watanabe, K. Okumura, Y. Takehana, S. Hirano and others. Thanks are extended to Dr. H. Yamazaki for providing data from trenching of the Atera fault conducted by Geological Survey of Japan, and Dr. H. Sakai for showing the results of the archeomagnetic dating at the Atotsugawa fault. Microearthquake data are supplied by Tottori Microearthquake Observatory and Kamitakara Observatory of Crustal Deformation, Disaster Prevention Research Institute, Kyoto University.

REFERENCES

AKI, K., Asperities, barriers, characteristic earthquakes and strong motion prediction, *J. Geophys. Res.*, **89**, 5867–5872, 1984.

DISASTER PREVENTION RESEARCH INSTITUTE, KYOTO UNIV., Trenches across the trace of the 1891 Nobi earthquake faults, *Rep. Coord. Comm. Earthq. Predict.*, **29**, 360–367, 1983 (in Japanese).

GEOLOGICAL SURVEY OF JAPAN, Exploratory excavation and fault activity of the Atera fault, central Japan, *Rep. Coord. Comm. Earthq. Predict.*, **28**, 299–303, 1982 (in Japanese).

GROUP FOR COMPILATION OF MICROSEISMICITY MAPS OF JAPAN, 1979, Microseismicity of Japan, *Rep. Coord. Comm. Earthq. Predict.*, **30**, 382–388, 1983 (in Japanese).

HIRANO, S. and T. NAKATA, Prehistoric large earthquakes deduced from fault activity along the Atera fault, central Japan, *Geogr. Rev. Japan*, **54**, 231–246, 1981 (in Japanese).

HIROOKA, K., Archeomagnetic study for the past 2,000 years in southwest Japan, *Mem. Fac. Sci., Kyoto Univ., Ser. Geol. and Mineral.*, **38**, 167–207, 1971.

HUZITA, K., Y. KISHIMOTO, and K. SHIONO, Neotectonics and seismicity in the Kinki area, *Geosciences, Osaka City Univ.*, **16**, 93–124, 1973.

JAPAN METEOROLOGICAL AGENCY, Catalog of relocated major earthquakes in and near Japan (1926–1960), *The Seismological Bulletin of the Japan Meteorological Agency Supplementary Volume No. 6*, 109 pp., 1982.

KANAMORI, H. and D. L. ANDERSON, Theoretical basis of some empirical relations in seismology, *Bull. Seism. Soc. Am.*, **65**, 1073–1095, 1975.

MATSUDA, T., Surface faults associated with Nobi (Mino-Owari) earthquake of 1891, Japan, *Spec. Rep. Earthq. Res. Inst., Univ. Tokyo*, **13**, 85–126, 1974 (in Japanese).

MATSUDA, T., Magnitude and recurrence interval of earthquakes from a fault, *Zisin (J. Seism. Soc. Japan)*, **28**, 269–282, 1975 (in Japanese).

MATSUDA, T., Relation between distribution of active faults and epicenters of damaging earthquakes on land, *Rep. Coord. Comm. Earthq. Predict.*, **24**, 282–285, 1980 (in Japanese).

MATSUDA, T., Active faults and damaging earthquakes in Japan—Macroseismic zoning and precaution fault zones, in *Earthquake Prediction—An International Reveiw*, Maurice Ewing Series 4, edited by D. W. Simpson and P. G. Richards, pp. 279–289, Am. Geophys. Union, 1981.

MIKUMO, T. and M. ANDO, A search into the faulting mechanism of the 1891 great Nobi earthquake, *J. Phys. Earth*, **24**, 63–87, 1976.

MIKUMO, T. and H. WADA, Atotsugawa fault and seismicity, *The Earth Monthly*, **5**, 325–334, 1983 (in Japanese).

NAKANE, K., Horizontal tectonic strain in Japan (I), (II), *J. Geod. Soc. Japan*, **19**, 190–199, 200–208, 1973 (in Japanese).

NISHIGAMI, K. and T. TSUKUDA, Generating process of a small earthquake, its foreshocks and aftershocks having a clustering structure, *Zisin (J. Seism. Soc. Japan)*, **35**, 523–537, 1982 (in Japanese).

OIKE, K., Seismic activities and crustal movements at the Yamasaki fault and surrounding regions in southwest Japan, *J. Phys. Earth*, **25**, S31–S41, 1977.

OKADA, A., Geomorphic development and fault topography in the Butai-Pass area along the Atera fault zone, central Japan, *Geogr. Rev. Japan*, **48**, 72–78, 1975 (in Japanese).

OKADA, A., M. ANDO, and T. TSUKUDA, Trenches across the Yamasaki fault in Hyogo prefecture, *Rep. Coord. Comm. Earthq. Predict.*, **24**, 190–194, 1980 (in Japanese).

OKADA, A., M. ANDO, and T. TSUKUDA, A recurrence interval of the Yamasaki fault, *Rep. Coord. Comm. Earthq. Perdict.*, **26**, 251–253, 1981a (in Japanese).

OKADA, A., M. ANDO, and T. TSUKUDA, Trenches, late holocene displacement and seismicity of the Shikano fault associated with the 1943 Tottori earthquake, *Disaster Prev. Res. Inst. Annu., Kyoto Univ.*, **24B**, 1–22, 1981b (in Japanese).

OKADA, A. and T. MATSUDA, A fault outcrop at the Onosawa pass and recent displacements along the Atera fault, central Japan, *Geogr. Rev. Japan*, **49**, 632–639, 1976 (in Japanese).

OMOTE, S., Aftershocks that accompanied the Tottori earthquake of Sept. 10, 1943, *Bull. Earthq. Res. Inst., Univ. Tokyo*, **33**, 641–661, 1955.

RESEARCH GROUP FOR ACTIVE FAULTS, *Active Faults in Japan: Sheet Maps and Inventories*, 363 pp., Univ. Tokyo Press, 1980a (in Japanese).

RESEARCH GROUP FOR ACTIVE FAULTS, Active faults in and around Japan: The distribution and the degree of activity, *J. Nat. Disaster Sci.*, **2**, 61–99, 1980b.

RESEARCH GROUP FOR EXCAVATION OF THE ATOTSUGAWA FAULT, Trenching excavation across the Atotsugawa fault, *The Earth Monthly*, **5**, 335–340, 1983 (in Japanese).

SAKAI, H. and K. HIROOKA, Fault movement derived from paleomagnetism, *The Earth Monthly*, **5**, 394–399, 1983 (in Japanese).

SCHWARTZ, D. P. and K. J. COPPERSMITH, Fault behavior and characteristic earthquakes: Examples from the Wasatch and San Andreas fault zones, *J. Geophys. Res.*, **89**, 5681–5698, 1984.

SHIMAZAKI, K. and T. NAKATA, Time predictable recurrence model for large earthquakes, *Geophys. Res. Lett.*, **7**, 279–282, 1980.

SIEH, K. E., Pre-historic large earthquakes produced by slip on the San Andreas fault at Pallet Creek, California, *J. Geophys. Res.*, **83**, 3907–3939, 1978a.

SIEH, K. E., Slip along the San Andreas fault associated with the great 1857 earthquake, *Bull. Seism. Soc. Am.*, **68**, 1421–1448, 1978b.

SIEH, K. E., A review of geological evidence for recurrence times of large earthquakes, in *Earthquake Prediction—An International Review*, Maurice Ewing Series 4, edited by D. W. Simpson and P. G. Richards, pp. 181–207, Am. Geophys. Union, 1981.

SUGIMURA, A. and T. MATSUDA, Atera fault and its displacement vectors, *Geol. Soc. Am. Bull.*, **81**, 2875–2890, 1965.

TAKEMURA, T., Active faults in Toyama prefecture, *The Earth Monthly*, **5**, 431–436, 1983 (in Japanese).

TAKEMURA, T. and S. FUJII, Active faults in the northern part of the Hida Mountains, central Japan,

The Quaternary Res., **22**, 297–312, 1983.

TOTTORI MICROEARTHQUAKE OBSERVATORY AND MICROEARTHQUAKE RESEARCH SECTION, DISASTER PREVENTION RESEARCH INSTITUTE, KYOTO UNIVERSITY, AND INSTITUTE OF EARTH SCIENCES, TOTTORI UNIVERSITY, Earthquake (M6.2) on Oct. 31, 1983 at the central part of Tottori Pref., *Rep. Coord. Comm. Earthq. Predict.*, **31**, 390–398, 1983 (in Japanese).

TSUKUDA, T., S. NAKAO, and Y. KISHIMOTO, Recent seismicity in the Tottori area, *Disaster Prev. Res. Inst. Annu., Kyoto Univ.*, **19B**, 1–12, 1976 (in Japanese).

TSUKUDA, T., V_P/V_S anomaly around the source region of the earthquake of M3.7 on September 30, 1977, in the vicinity of the Yamasaki fault, *Disas. Prev. Res. Inst. Annu., Kyoto Univ.*, **21B**, 27–36, 1978 (in Japanese).

TSUKUDA, T., Microearthquakes along the Atotsugawa fault, *The Earth Monthly*, **5**, 417–425, 1983 (in Japanese).

TSUYA, H., The Shikano and Yoshioka faults and geological features around them—Geological observation with respect to the Tottori earthquake of Sep. 10, 1943, *Bull. Earthq. Res. Inst., Univ. Tokyo*, **22**, 1–32, 1944 (in Japanese).

USAMI, T., *Descriptions of All Disastrous Earthquakes*, 327 pp., Univ. Tokyo Press, 1975 (in Japanese).

WESNOUSKY, S. G., C. H. SCHOLZ, K. SHIMAZAKI, and T. MATSUDA, Earthquake frequency distribution and the mechanics of faulting, *J. Geophys. Res.*, **88**, 9331–9340, 1983.